

## Numerical Study on Ductility and Energy Dissipation of High-rise Composite Shear Walls

Amirhoshang Akhayeissy<sup>a</sup>, Kambiz Daneshvar<sup>a\*</sup>, Morteza Amooie<sup>b</sup>, Dina Ghazi-Nader<sup>a</sup>

<sup>a</sup> Department of Civil Engineering, Razi University, Kermanshah, Iran

<sup>b</sup> Department of Civil Engineering, Islamic Azad University South Tehran Branch, Tehran, Iran

### Keywords

Composite shear walls,  
Ductility,  
Energy dissipation,  
Finite element analysis,  
OpenSees.

### Abstract

Shear walls are used in buildings as a lateral load resisting system. In recent years, research on seismic behavior of composite steel-concrete shear walls has increased. The seismic behavior of shear walls is characterized by strength, ductility, and energy dissipation capacity. The objective of this study is to investigate the effect of some parameters including the height of the wall, compressive strength of concrete and reinforcement ratio on ductility and energy dissipation of composite shear walls. To do so, twelve specimens of high-rise composite shear walls under cyclic loading have been modeled. Finite element method has been carried out via OpenSees software to simulate shear walls. The results indicate that Concrete compressive strength and height of the wall have no significant effect on the ductility of composite shear walls, and increasing the reinforcement ratio reduces the ductility. In addition, it is observed that increasing the reinforcement ratio and height of shear wall increases energy dissipation, and the effect of concrete strength on increasing the energy dissipation of the wall is very low. The effect of reinforcement ratio on energy dissipation is greater than that of ductility.

### 1. Introduction

Shear walls play an outstanding role in providing the lateral stiffness of the buildings and enhance the stability during seismic events.

In recent years, the use of Composite walls has increased due to the performance characteristics when subjected to loads and having higher safety. Composite steel-concrete walls (CSRCW) are reinforced concrete walls with steel encased profiles that are located at the boundary regions. The boundary elements of shear walls carry the majority of forces under the applied loads. In traditional system that used boundary element reinforcement, large number of vertical reinforcements must be confined by sufficient hoops, which complicates construction and on the other hand, is difficult to place these boundary reinforcements in a wall with low thickness. For these reasons, steel profiles replaced the boundary element reinforcement.

Different types of shear wall systems through both experimental and analytical have been studied by researchers [1-5]. Dan et al. [6] carried out experimental and theoretical studies on composite shear walls with steel encased profiles. The shear walls showed higher energy

dissipation and initial stiffness with increasing amount of steel. Wang et al. [7] experimentally investigated the seismic behavior, including failure phenomena, failure mechanism, load carrying capacity, ductility and energy dissipation characteristics of steel plate reinforced concrete composite shear walls and compared it to the traditional RC shear walls. The composite walls were found to have better seismic performance than the traditional RC shear walls. In addition, the results showed that the thickness of the wall is the most important parameter to increase ductility and energy dissipation capacity. Darban and Kalantary [8] conducted a study about Lateral Pressure on Rigid Retaining Walls without Lateral Movement. Vertical stress distribution in the vicinity of a surface perpendicular to the fixed horizontal position that models the rigid retaining walls behavior was investigated, and the results have been compared with the recent studies findings. Dey and Bhowmick [9] conducted a study on concrete stiffened steel plate shear wall. Good ductility, initial elastic stiffness and shear capacity of this system under time-history analysis was observed. Some different types of shear wall formed by inserting the steel plates and steel section were proposed and investigated by Gan et al. [10]. It was observed that Such types of walls have

\* Corresponding Author:

E-mail address: [Daneshvar2@yahoo.com](mailto:Daneshvar2@yahoo.com) – Tel, (+98) 9112829349

Received: 05 October 2018; Accepted: 28 December 2018

shown quite larger shear stiffness compared to traditional reinforced concrete walls.

The aim of this work is to investigate effects of some parameters such as wall height, concrete compressive strength and Reinforcement ratio on seismic behavior of composite steel-concrete shear walls. To this end, the hysteresis curves of one sample of shear walls have been verified with experimental data by using OpenSees software [11] and twelve composite shear walls with heights of 21, 24 and 27 meters, two compressive strength of concrete equal to 25 and 35 Mpa, and Reinforcement ratio of 1% and 2% have been considered.

## 2. Numerical Modeling and Verification

Commercial finite element software OpenSees was employed for simulation and nonlinear analyses in this study. One sample of shear walls of DAN research [6] that shows in Figure 1 was modeled to validate the finite element modeling.

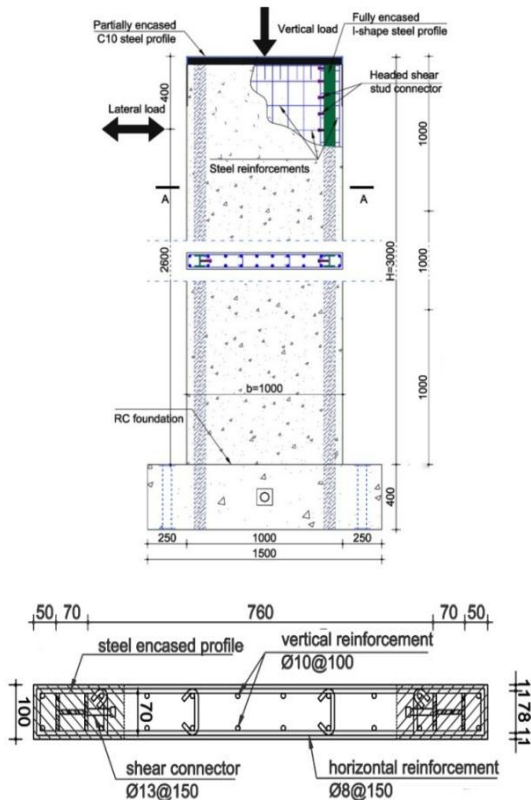


Figure 1. Details of the composite shear wall

The values of yield strength ( $f_y$ ), ultimate strength ( $f_u$ ), modulus of elasticity ( $E_s$ ) of steel are 328,516 and  $2.03 \times 10^5$  Mpa, respectively. Concrete with the average cube strength of 62Mpa and young modulus of 38.031 Mpa was adopted, according to reference article. The displacement based (stiffness) fiber element model that is an accurate method for nonlinear analysis of structures used for analysis of shear walls in this study. The base of the wall, or in other words, wall connection to the foundation was modeled using the ZeroLengthSection element. This element at the end of a beam-column element can incorporate the fixed-end rotation caused by strain penetration to the beam-column element [12]. The displacement based-Stiffness method uses

displacement interpolation function. It accounts for axial and transverse displacements of the elements. The most commonly used function for the beam-column elements are cubic hermitian polynomial and Linear Lagrangian shape function. The element force and deformation vectors can be calculated as [13]

$$P = [P1, P2, P3, \dots P6]^T \quad (1)$$

$$U = [U1, U2, U3, \dots U6]^T \quad (2)$$

and force and deformation vectors of the section are given by:

$$q(X) = [N(X), M(X)]^T \quad (3)$$

$$V_S(X) = [\epsilon_0(X), \phi(X)]^T \quad (4)$$

where  $N$  is the axial force,  $M$  is the bending moment,  $\epsilon_0$  is axial strain and  $\phi$  is the curvature with respect to section position 'x'. The element force and deformations are shown in Figure 2.

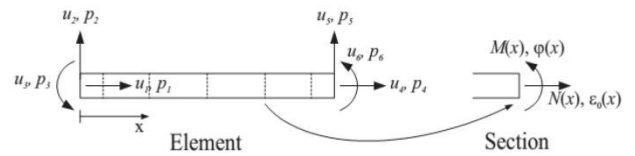


Figure 2. Element force and deformations

A numerical model for shear wall is shown in Figure 3. In order to reduce the possibility sliding between steel and concrete, the connection between these two materials is accomplished with shear studs that welded to the steel profiles. Concrete 02 was used for the unconfined and confined concrete based on the Chang and Mander model [14] as shown in Figure 4 (a).

In order to increase the accuracy of the modeling, the effects of the probable slipping of the reinforcing steel were considered. The BondSP01 model provided in OpenSees for simulating the bond-slip mechanism. Figure 4 (c) shows the bond-slip material presented by Zhao and Sritharan [15], that developed based on the pull-out tests results of deformed steel reinforcing bars anchored in concrete footings with sufficient embedment length. The lateral load versus lateral displacement hysteresis curve for the specimen is compared with numerical result of the present work (Figure 5). As can be seen, the FE numerical response shows a good agreement with the experimental result. Therefore, numerical modeling based on fiber method can be used to examine shear walls behavior.

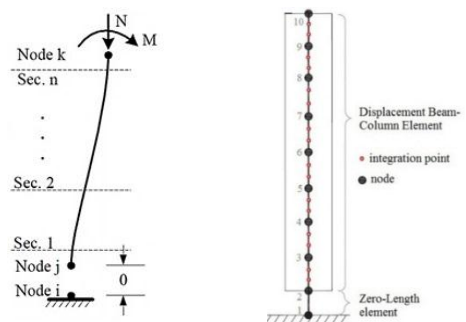


Figure 3. Numerical model for shear wall

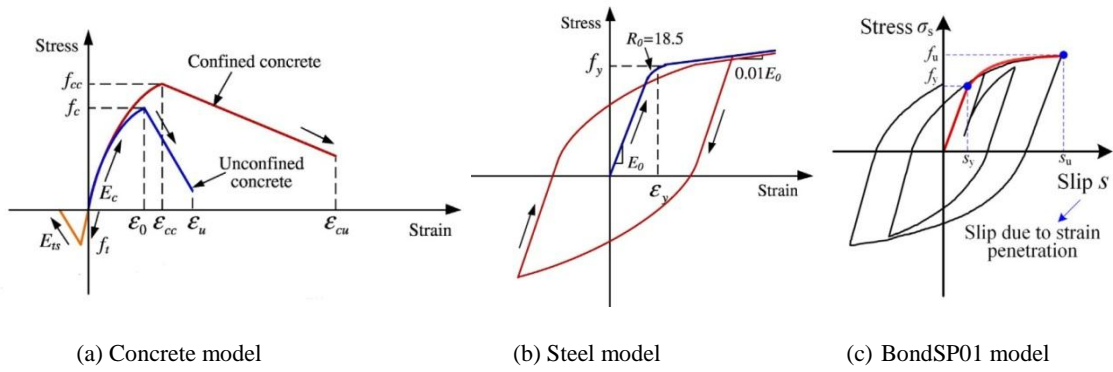


Figure 4. Material models

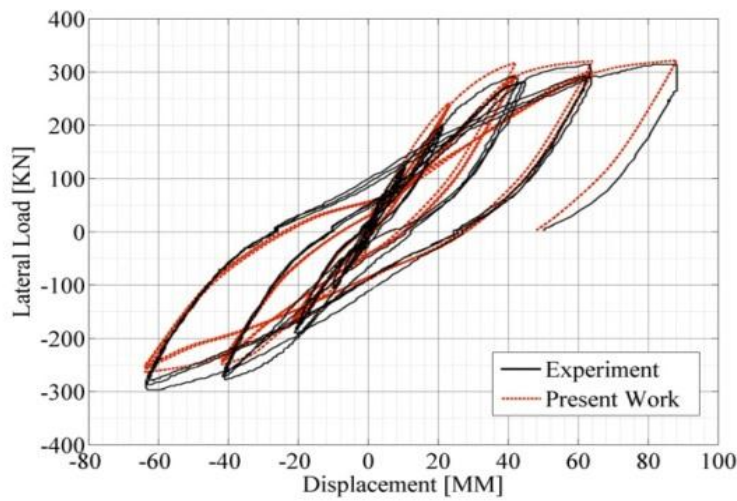
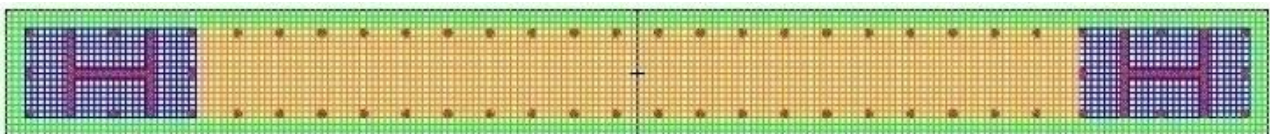


Figure 5. Comparison of numerical hysteresis curve with experimental result.

### 3. Nonlinear Analysis of High-rise Shear Walls

Twelve specimens of high-rise composite shear walls were modeled. Three parameters including height of wall, compressive strength of concrete and reinforcement ratio of specimens were adopted. The specimens were named according to these parameters. Specifications of shear walls are presented in Table 1 and material properties adopted in numerical model presented in Table 2. The length of each BeamColumn element was adopted 75 cm. Accordingly, the walls with a height of 21, 24 and 27 meters were simulated

by 28, 32 and 36 Nonlinear BeamColumn element, respectively. Ten integration points were utilized per element. As seen in Figure 6, cross section of the wall is discretised into a number of fibres and each fibre is linked to a material representation such as confined concrete in the boundary element, confined concrete in wall web, unconfined concrete in cover, and steel. All wall specimens were analyzed under constant vertical load and cyclically increasing lateral loads. The loading sequence is in the form of displacement-control protocol as shown in Figure 7 which was incremented in steps of 5 mm until failure.



- Confined concrete in the boundary element
- Confined concrete in wall web
- Unconfined concrete
- Steel

Figure 6. Fiber sections for shear walls

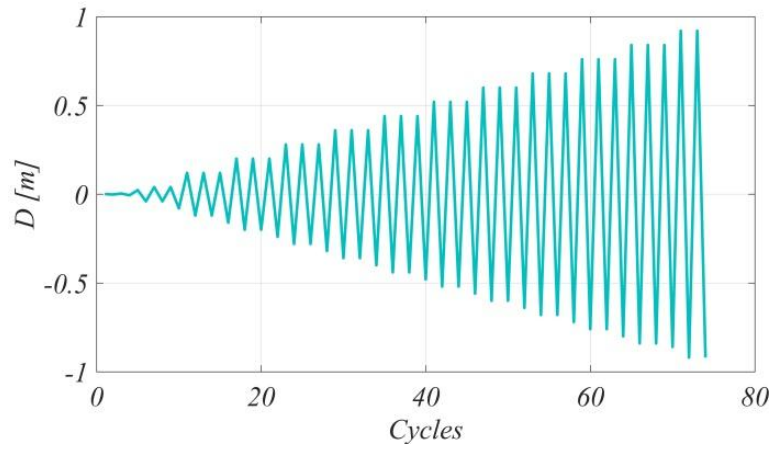


Figure 7. Loading history

Table 1. Specifications of shear walls adopted in numerical modeling.

Specimen	$h_w$ (cm)	$l_w$ (cm)	$b_w$ (cm)	$\rho$	$f'_c$	Dbe	Lrbe	Lrw
W1-f25r1	2100	300	30	1%	25	30x40	20Φ8	20Φ20@10.5
W1-f35r1					35			
W1-f25r2				2%	25		14Φ8	14Φ21@10
W1-f35r2					35			
W2-f25r1	2400			1%	25		20Φ8	20Φ20@10.5
W2-f35r1					35			
W2-f25r2				2%	25		14Φ8	14Φ21@10
W2-f35r2					35			
W3-f25r1	2700			1%	25		20Φ8	20Φ20@10.5
W3-f35r1					35			
W3-f25r2				2%	25		14Φ8	14Φ21@10
W3-f35r2					35			

Note:  $h_w$ =wall height,  $l_w$ =wall length,  $b_w$ =wall thickness,  $\rho$ = Reinforcement ratio,  $f'_c$ = Compressive strength of concrete, Dbe= Dimensions of the boundary element, Lrbe= Longitudinal reinforcement of the boundary element, Lrw= Longitudinal reinforcement of web.

Table 2. Material properties

Concrete	compressive strength	tensile strength	Young's modulus	yield strain	ultimate strain
	$f'_c$ (Mpa)	$f'_t$ (Mpa)	$E_c$ (KN/mm <sup>2</sup> )	$\epsilon_c$ (%)	$\epsilon_u$ (%)
	25,35	2,2.88	24.27	0.2	0.5
Reinforcement steel	yielding strength	ultimate strength	Young's modulus	hardening strain	ultimate strain
	$f_y$ (Mpa)	$f_{su}$ (Mpa)	$E_s$ (KN/mm <sup>2</sup> )	$E_{sh}$ (KN/mm <sup>2</sup> )	$\epsilon_u$ (%)
	400	500	200	3.33	3
Profile steel	240	400	200	3.33	3

### 3.1. Hysteresis Response

The lateral load versus lateral displacement hysteresis curves for all the specimens are depicted in Figure 8. It can be seen from the results that Residual displacements occurred after the elastic limit and curves descended stably in the failure stage; hence all specimens show a ductile behavior.

## 4. Results and Discussion

### 4.1. Ductility

The plastic deformation and ductility is the ability of members to develop their ultimate load carrying prior to failure. The displacement ductility coefficient is an important index for evaluating the plastic deformation capacity.

Ductility coefficient is evaluated as Eq. (5)

$$\mu\Delta = \frac{\Delta u}{\Delta y} \tag{5}$$

where  $\Delta y$  is the yield displacement, and  $\Delta u$  is the ultimate displacement.

The MBBE method (method based on balance of energy) was adopted to get the value of the yield displacement [16]. Based on this method, the idealization of the load-displacement diagram is performed through an energy balance. To obtain the yield displacement, the OA line (Figure 9) should be drawn in such a way as area A1 be matched with area A2. And ultimate displacement is defined when a reduction of 15% of the maximum load is reached in the descending branch.

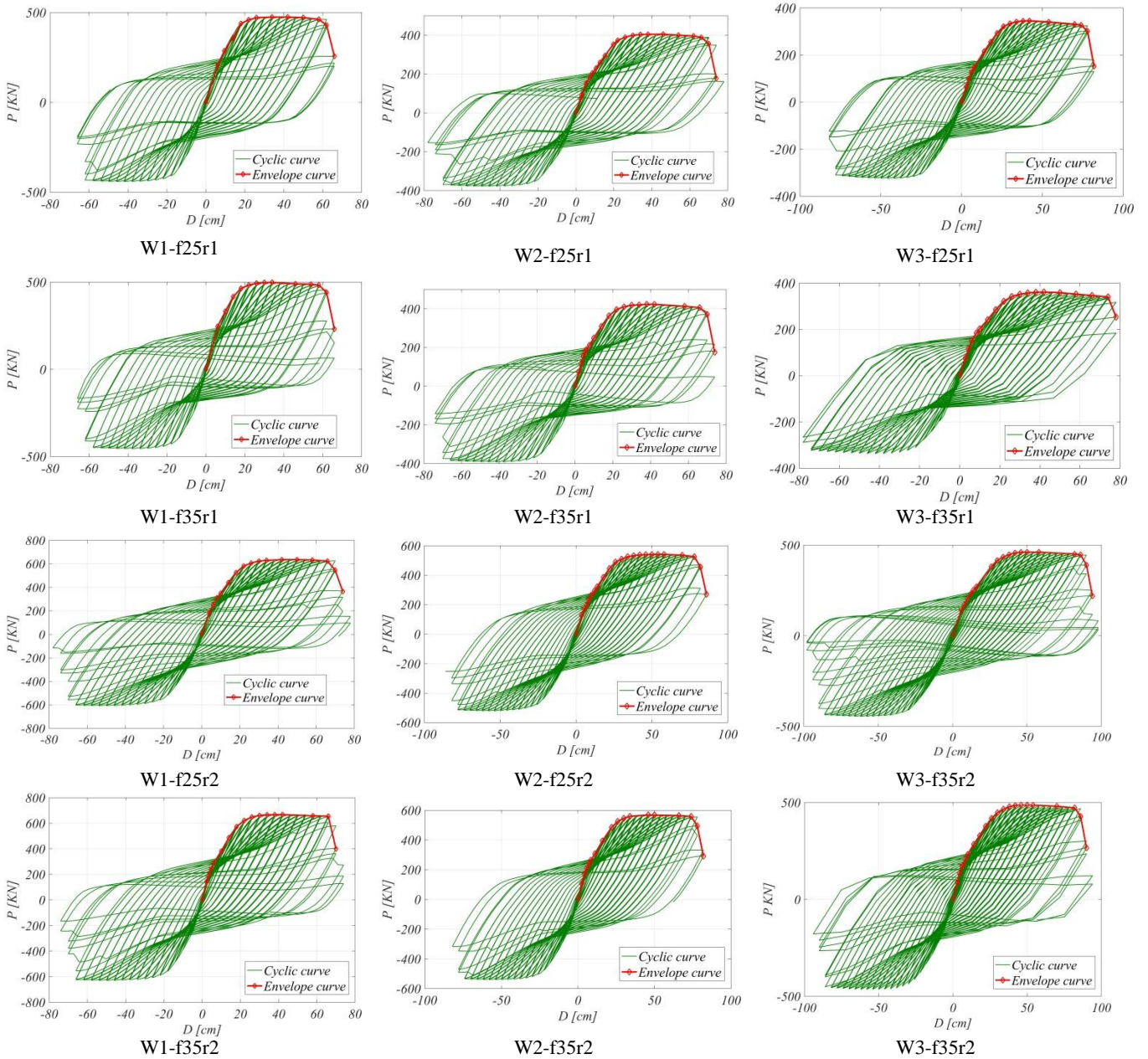


Figure 8. Lateral force-displacement hysteresis curves of specimens.

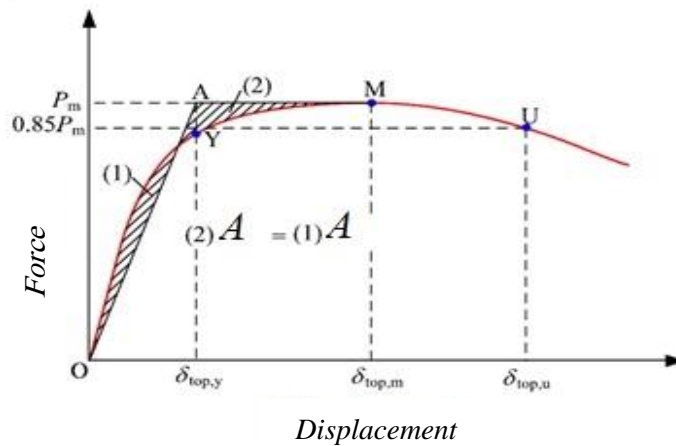


Figure 9. Definition of yield and ultimate displacement

The load displacement curves of the walls were taken from their hysteresis curves (Figure 10). Idealization of load-displacement curves was done by coding in MATLAB software; based on the above method, the diagrams of W1 specimens have been shown for example (Figure 11). The values of yield and ultimate displacement were extracted from them (Table 3). The ductility coefficients of specimens are compared in Figure 12. According to the results, it is evident that concrete compressive strength and wall height

have no significant effect on the ductility of shear walls. The doubling of the reinforcement ratio causes approximately about 10 % reduction in the walls ductility. Figure 13 describes variations of ductility with reinforcement ratio. The ductility coefficient of shear wall specimens is between 3.1 and 4, among which the highest ductility is related to sample w1-f35r1 and the lowest ductility is related to w3-f35r2.

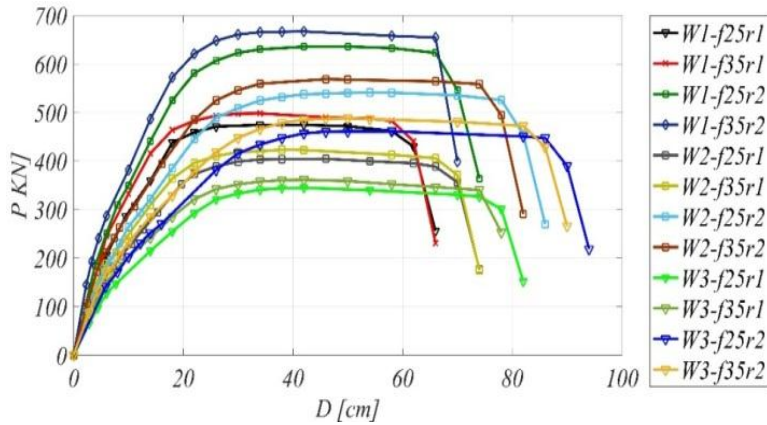


Figure 10. Force-displacement curves of specimens.

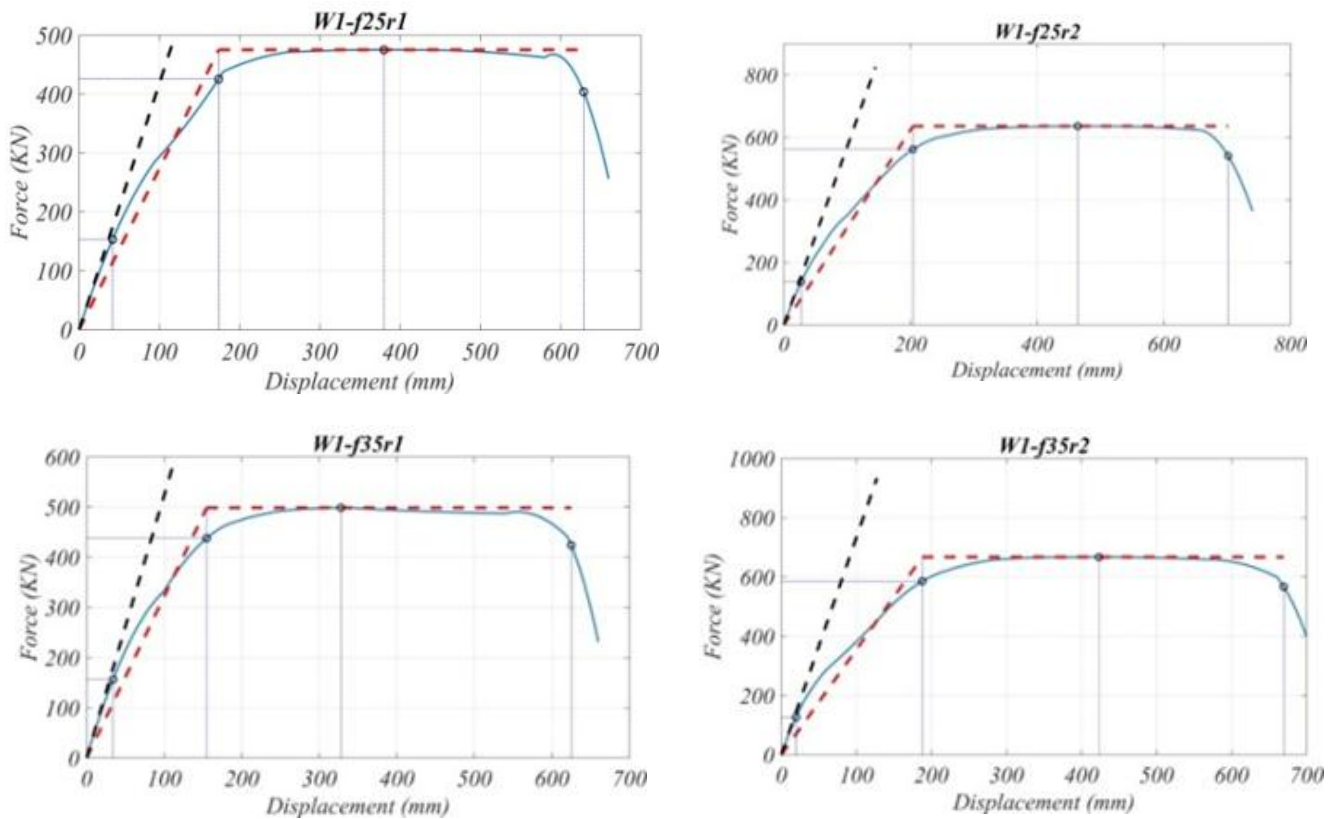
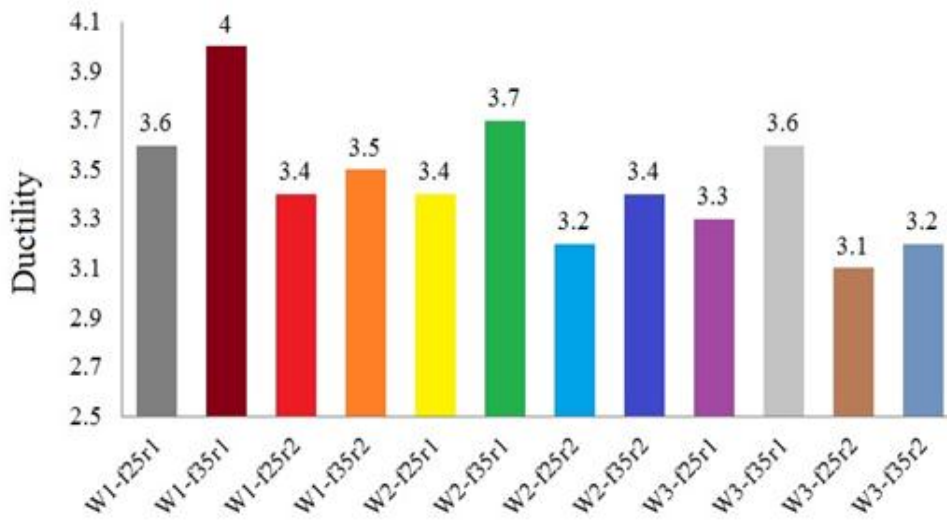


Figure 11. Load-displacement curve Idealization with MBBE.

**Table 3.** Ductility coefficient of specimens

	YELDING		ULTIMATE		Ductility
	Force (KN)	Dis. (mm)	Force (KN)	Dis. (mm)	
W1-f25r1	173.9	425.4	628.7	403.7	3.6
W1-f35r1	154.8	437.8	625	423.7	4
W1-f25r2	204	562.2	701.5	540.9	3.4
W1-f35r2	187.9	585.1	669.5	567	3.5
W2-f25r1	203	358.2	705	344.2	3.4
W2-f35r1	186.7	370.9	703.6	359.9	3.7
W2-f25r2	250.9	480.7	818.4	459.9	3.2
W2-f35r2	230.4	497.7	783.4	483.8	3.4
W3-f25r1	233.5	303.7	783.9	293.3	3.3
W3-f35r1	210.7	313.9	760	307.2	3.6
W3-f25r2	286.9	406	461.4	899.2	3.1
W3-f35r2	266.1	423.8	865.6	414.7	3.2



**Figure 12.** Comparative ductility

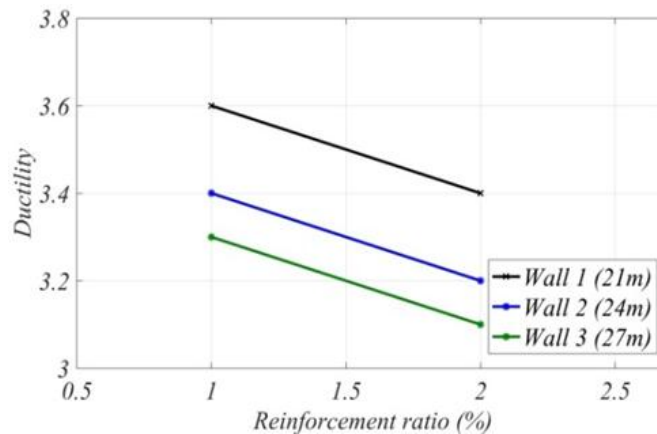


**Figure 13.** Variation of ductility with reinforcement ratio

**4.2. Energy Dissipation**

As previously stated the cyclic behavior of reinforced concrete members is characterized by strength, ductility, and energy dissipation capacity. A energy dissipation process is a process in which energy decreases. The dissipated energy is an important factor in the earthquake resistance estimation. There are many design parameters that affect the energy dissipation of a reinforced concrete member such as the reinforcement ratio, reinforcement arrangement, magnitude of plastic deformation, and

magnitude of axial compressive force and etc [17]. Numerous experimental and numerical studies have been conducted to evaluate the energy capacity of reinforced concrete members. Some researchers presented empirical methods for predicting the energy dissipation, without considering the design parameters of the structure [18-21]. In the Park and Eom study [22], simplified equations were developed to evaluate the energy dissipation of walls, and the effects of design parameters such as the cross-section type, shear span-to-height ratio, reinforcement detail and axial force on the energy dissipation were considered.

According to Park and Eom study, the total energy dissipated can be evaluated as Eq. (6)

$$E = E_I + \sum E_{II} \tag{6}$$

where  $E_I$  , is the area under the overall envelope curve and  $E_{II}$  , is the area enclosed by a cyclic curve. These areas are shown in Figure 14.

Based on what was said the energy dissipation of the walls were calculated and the values are compared in the figure15 .It can be seen that the values of energy dissipation of specimens are between 7953 and 14900(KN.m). From

the results, it can be drawn that the energy dissipation of walls is improved, as the height increases. When the wall height is increased 3 meters and 6 meters, energy dissipation increases about 3% and 15%, respectively. When the reinforcement ratio increases from 1% to 2%, energy dissipation increase about 60%.For example the energy dissipation of w1-f25r2 is 58% higher than w1-f25r1.As depicted,the wall with higher compressive strength concrete dissipated more energy, but this increase is negligible. w1-f25r1 and w3-f3r2 specimens has the lowest and highest energy dissipation, respectively.

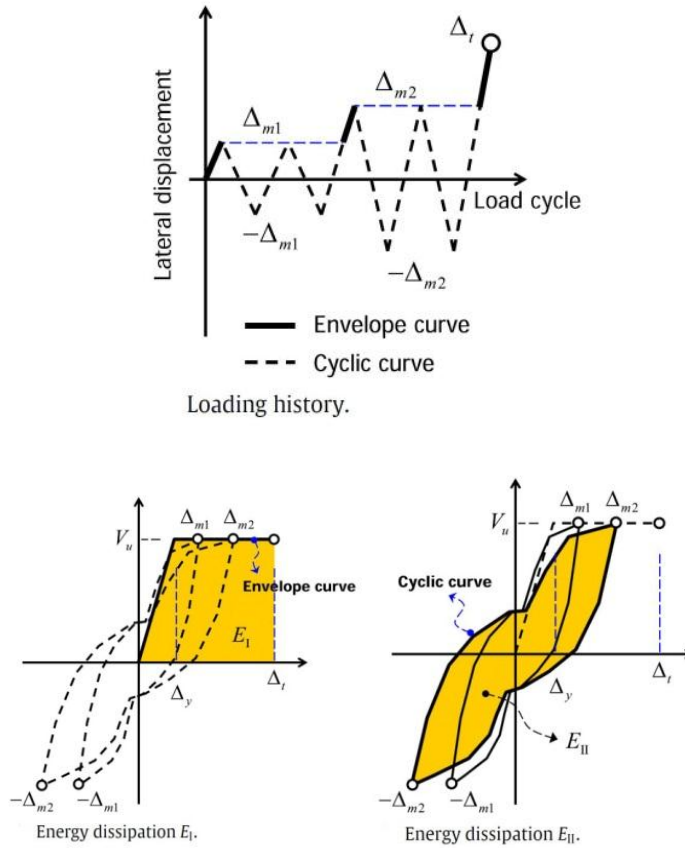


Figure 14. Classification of energy dissipation

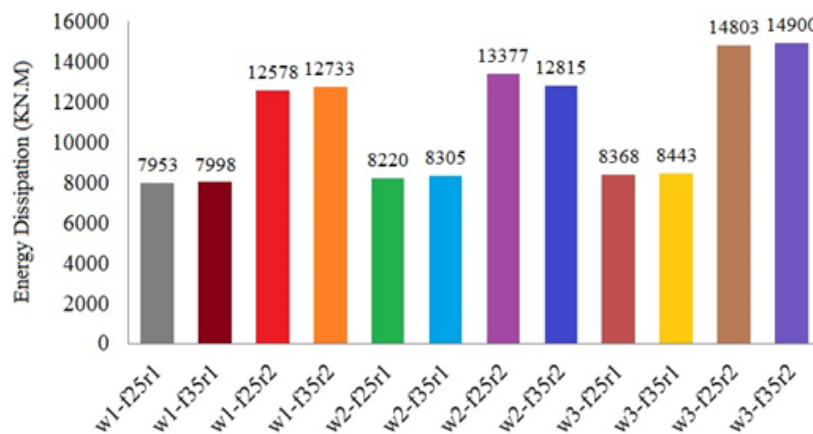


Figure 15. Comparative dissipated energy

## 5. Conclusions

In this work, the ductility and energy dissipation of composite shear walls with various heights, concrete compressive strengths and reinforcement ratios, under constant vertical load and cyclically increasing lateral loads were investigated through numerical modeling with OpenSees. The conclusions can be drawn as:

1. Concrete compressive strength and height of wall have no significant effect on ductility of composite shear walls.
2. Increasing the energy absorption of the wall by increasing the compressive strength of the concrete is negligible, on the other hand it can be said that, The effect of concrete strength on the energy absorption of the composite shear wall is very low. From the results it can be drawn that the energy dissipation of composite shear wall is improved, as the height of wall increases.
3. When the reinforcement ratio increases from 1% to 2%, the ductility decrease about 10%, and energy dissipation increase about 60%, hence it can be said that Increasing the reinforcement ratio, reduces the ductility and increases energy dissipation. and it is observed that the effect of reinforcement ratio on energy dissipation is greater than that of ductility.
4. Among the three parameters of concrete compressive strength, wall height and reinforcement ratio; concrete strength has the lowest effect and reinforcement ratio has the highest effect on seismic behavior including ductility and energy dissipation of shear walls.

## References

- [1] F. Y. Liao, L. H. Han, Z. Tao, Experimental behavior of RC shear walls framed with steel reinforced concrete (SRC) columns under cyclic loading. In *Steel and Composite Structures: Proceedings of the 4th International Conference on Steel and Composite Structures (ICSCS10)*, Sydney, Australia, (2010).
- [2] W. K. Saari, J. F. Hajjar, A. E. Schultz, C. K. Shield, Behavior of shear studs in steel frames with reinforced concrete infill walls, *Journal of Constructional Steel Research* 10 (2004) 1453–1480.
- [3] A. Astaneh-Asl, *Seismic behavior and design of composite steel plate shear walls*. Moraga, CA: Structural Steel Educational Council, (2002).
- [4] J. Qian, Z. Jiang, X. Ji, Behavior of steel tube-reinforced concrete composite walls subjected to high axial force and cyclic loading, *Engineering Structures* 5 (2012) 173–184.
- [5] X. Tong, J. F. Hajjar, A. E., C. K. Shield, Cyclic behavior of steel frame structures with composite reinforced concrete infill walls and partially-restrained connections, *Journal of Constructional Steel Research* 4 (2005) 531–552.
- [6] D. Dan, A. Fabian, V. Stoian, Theoretical and experimental study on composite steel–concrete shear walls with vertical steel encased profiles, *Journal of Constructional Steel Research* 5 (2011) 800–813.
- [7] W. Wang, Y. Wang, Z. Lu, Experimental study on seismic behavior of steel plate reinforced concrete composite shear wall. *Engineering Structures* 160 (2018) 281–292.
- [8] R. Darban, F. Kalantary, Lateral Pressure on Rigid Retaining Walls without Lateral Movement, *Computational Research Progress in Applied Science & Engineering (CRPASE)* 1 (2015) 29–37.
- [9] S. Dey, A. K. Bhowmick, Seismic performance of composite plate shear walls, In *Structures* 6 (2016) 59–72.
- [10] L. X. Gan CJ, W. Wang, Seismic behavior of steel plate reinforced concrete shear walls, 14th world conference on earthquake engineering, (2008).
- [11] Open system for earthquake engineering simulation (OpenSees). <http://opensees.berkeley.edu/>.
- [12] J. Melo, C. Fernandes, H. Varum, H. Rodrigues, A. Costa, A. Arêde, Numerical modelling of the cyclic behaviour of RC elements built with plain reinforcing bars, *Engineering structures* 2 (2011) 273–286.
- [13] S. T. John, Implementation of Fiber Element Model for Non-Linear Analysis (Doctoral dissertation), (2015).
- [14] G.A. Chang, J.B. Mander, Seismic energy based fatigue damage analysis of bridge columns: part 1 – evaluation of seismic capacity, National Center for Earthquake Engineering Research (NCEER), 1994.
- [15] J. Zhao, S. Sritharan, Modeling of strain penetration effects in fiber-based analysis of reinforced concrete structures, *ACI structural journal*, 2 (2007) 192–202.
- [16] A. C. Barrera, J. L. Bonet, M. L. Romero, M. A. Fernández, Ductility of slender reinforced concrete columns under monotonic flexure and constant axial load, *Engineering Structures* 40 (2012) 398–412.
- [17] H. Park, T. Eom, A simplified method for estimating the amount of energy dissipated by flexure-dominated reinforced concrete members for moderate cyclic deformations, *Earthquake Spectra* 2 (2006) 459–490.
- [18] M. J. N. Priestley, Performance based seismic design, *Bulletin of the New Zealand society for earthquake engineering* 3 (2000) 325–346.
- [19] Y.Y. Lin, M.H. Tsai, J.S. Hwang, K.C. Chang, Direct displacement-based design for building with passive energy dissipation systems, *Engineering Structures* 1 (2003) 25–37.
- [20] M. S. Medhekar, D. J. L. Kennedy, Displacement-based seismic design of buildings—theory, *Engineering structures* (2000) 201–209.
- [21] Y.Y. Lin, E. Miranda, Evaluation of equivalent linear methods for estimating target displacements of existing structures, *Engineering structures* 12 (2009) 3080–3089.
- [22] T. S. Eom, H.G. Park, Evaluation of energy dissipation of slender reinforced concrete members and its applications, *Engineering Structures* 9 (2010) 2884–2893.